

ABSTRACT: The aim of this study was to investigate motor unit (MU) characteristics of the biceps brachii in poststroke patients using high-density surface electromyography (sEMG). Eighteen chronic hemiparetic stroke patients took part. The Fugl-Meyer score for the upper extremity was assessed. Subjects performed an isometric step contraction consisting of force levels from 5%–50% maximal voluntary contraction while sEMG of the biceps brachii was recorded with a two-dimensional 16-channel electrode array. This was repeated for both sides. Motor unit action potentials (MUAPs) were extracted from the EMG signals, and their root-mean-square value (RMS_{MUAP} , reflecting MU size) and mean frequency of the power spectrum ($FMEAN_{MUAP}$, reflecting recruitment threshold) were calculated. $FMEAN_{MUAP}$ was smaller on the affected than on the unaffected side, indicating an increased contribution of low-threshold MUs, possibly related to degeneration of high-threshold MUs. The ratio of RMS_{MUAP} on the affected side divided by that on the unaffected side correlated significantly with the Fugl-Meyer score. This ratio may reflect the extent to which reinnervation has occurred on the affected side.

Muscle Nerve 39: 177–185, 2009

MOTOR UNIT PROPERTIES OF BICEPS BRACHII IN CHRONIC STROKE PATIENTS ASSESSED WITH HIGH-DENSITY SURFACE EMG

LAURA A.C. KALLENBERG, PhD, and HERMIE J. HERMENS, PhD

Roessingh Research and Development, P.O. Box 310, 7500 AH Enschede, The Netherlands

Accepted 20 May 2008

As a consequence of a stroke, motor control of one or more extremities on one side of the body may be affected. Spasticity may occur, control of a number of motor units of the affected muscles may be lost (paresis), and voluntary motor control of the remaining motor units may change.

Many researchers have investigated muscle activation and coordination patterns after stroke. Weakness,⁸ abnormal co-contraction of antagonistic muscles,⁸ abnormal co-activation patterns,^{12,26} muscle fatigue,⁴⁶ and delays in initiation and termination of muscle activity^{7,12,28} have been reported.

However, knowledge about changes in properties and control of motor units (MUs) after a stroke is still limited. Some evidence for changes in MU prop-

erties is provided by electrophysiological studies in poststroke subjects.⁴⁷ MU degeneration has been reported to occur as early as 2 weeks after stroke,²⁹ and it appears to affect mainly type II fibers.^{6,9,11,14,19,43} This was attributed to disuse atrophy of type II fibers, in combination with an overuse of type I fibers related to rigidity.¹⁹ Some authors have suggested transsynaptic degeneration (atrophy of spinal motoneurons following damage to the upper motoneurons of the corticospinal tract that make synaptic connections to them) in type II motoneurons.^{9,11,26,37} Other authors suggest that the remaining MUs enlarge during the chronic stage of stroke due to collateral sprouting and branching of the motor neurons.^{9,10,28,35} In this process, type II muscle fibers may become connected to type I motor neurons, which leads to a transformation of these fibers to type I. Accordingly, an increased MU fiber density was found on the affected side of subjects with hemiplegia.¹⁰

So far, MU characteristics after a stroke have been investigated using intramuscular EMG recordings. Recently, extensive experience has been gained with high-density surface EMG (sEMG) recordings that enable us to noninvasively assess MU properties. Such recordings are obtained by placing an array of

Abbreviations: BMI, body mass index; $FMED_G$, global median frequency of the power spectrum; $FMEAN_{MUAP}$, mean frequency of the power spectrum of a motor unit action potential; MR, motor unit action potential rate; MU, motor unit; MUAP, motor unit action potential; MVC, maximal voluntary contraction force; RMS_G , global root-mean-square value; RMS_{MUAP} , root-mean-square value of the motor unit action potential; sEMG, surface electromyography

Key words: motor unit action potentials; motor unit characteristics; stroke patients; high-density surface EMG; multichannel array EMG

Correspondence to: L.A.C. Kallenberg; e-mail: l.kallenberg@rrd.nl

© 2008 Wiley Periodicals, Inc.

Published online 25 November 2008 in Wiley InterScience (www.interscience.wiley.com). DOI 10.1002/mus.21090

small, closely spaced electrodes on the skin above the muscle of interest. From these recordings, motor unit action potentials (MUAPs) can be distinguished and extracted and their propagation along the muscle fibers can be tracked.^{25,32,44}

One- or two-dimensional electrode arrays have been used to investigate various physiological and pathophysiological phenomena.^{20,23,38,41,42,45} Ramaekers et al.⁴⁰ demonstrated increased MUAP size in patients with spinal muscle atrophy and decreased MUAP size in patients with Duchenne muscular dystrophy compared with healthy controls. Kallenberg et al.³⁴ showed that variables obtained with high-density sEMG showed differences between cases with chronic neck-shoulder pain and healthy controls, while conventional EMG variables did not show such differences. With high-density sEMG, Drost et al.¹⁶ were able to demonstrate that MU size is larger in postpolio patients. A recent review of clinical applications concluded that high-density sEMG is suitable for investigation of changes in neurogenic disorders.¹⁷

To further extend the understanding of the consequences of a stroke, the aim of this study was to investigate MU characteristics of the biceps brachii in poststroke subjects with high-density sEMG. Because of the large intersubject variability of the sEMG signal caused by several anatomical and physiological factors,²¹ this study focused on intrasubject differences between the affected and the unaffected side. High-density sEMG recordings were performed on the biceps brachii muscles of both sides during a step contraction with increasing force levels from 5%–50% of the maximal voluntary contraction force (MVC).

MATERIALS AND METHODS

Subjects. Eighteen hemiparetic stroke patients recruited from the rehabilitation center “Het Roesingh” in Enschede, the Netherlands, were included in the study if they had a first unilateral ischemic stroke and sufficient cognitive abilities to understand spoken instructions. Demographic characteristics of the population are presented in Table 1.

Subjects had to be at least 6 months poststroke and had to be able to move their arm against gravity (Medical Research Council score for biceps brachii ≥ 3). Passive shoulder abduction to at least 70° had to be possible without pain. Exclusion criteria were the presence of additional orthopedic diseases of the upper extremities, psychiatric comorbidity, hypersensitivity, shoulder-hand syndrome, and use of antispastic medication. All subjects signed an informed

Table 1. Population characteristics.

Characteristic	
Sex	12 men, 6 women
Age (years)	64 (39–78)
Weight (kg)	80 (55–155)
Height (cm)	176 (158–184)
Body mass index (kg/m ²)	25.7 (21.6–34.8)
Time since stroke (years)	2 (0.5–10)
Affected side	11 left, 7 right
Fugl-Meyer score	35.5 (9–62)
Ashworth score	2 (0–4)

Median values and ranges (in parentheses) are reported. Fugl-Meyer score: clinical scale for motor recovery (upper extremity part, maximum value 66). Ashworth score: clinical scale for muscle tone in the elbow flexors (maximum value 4).

consent. The study was approved by the local medical ethics committee and experiments were performed in accordance with the Helsinki Declaration of 1975.

General Procedures. The protocol started with assessment of the upper extremity portion of the Fugl-Meyer score for motor recovery after stroke.²⁴ Subsequently, the Ashworth scale for muscle tone was scored for the elbow flexors.⁴

Muscle activity of the biceps brachii and force were recorded simultaneously. The protocol was first performed at the unaffected side and was repeated for the affected side.

Subjects were seated next to a height-adjustable table with their lower arm placed in a device that measured isometric elbow flexion and extension forces. The position of the upper arm was adjusted to optimize torque production, e.g., the arm was abducted to 70° while it remained in the plane of the trunk, the elbow was flexed to $\approx 90^\circ$, and the wrist was in a neutral position (midway between pronation and supination). Deviation of $\pm 10^\circ$ of the elbow angle, e.g., due to joint rigidity, was allowed since it was not expected to influence the results. The lower arm was supported by the device.

For determination of the MVC, subjects were asked to perform a maximal contraction three times with 2 min rest in between. Verbal encouragement as well as real-time feedback of the force level was provided. When the third measurement was more than 10% higher than the highest of the first two, a fourth and, if necessary, fifth measurement was performed. The force signal was averaged with a 100 ms moving window. The maximum value was taken as the MVC. Force feedback was provided on a screen in front of the subject. The gain of the force feedback was adapted such that deviations of 1 N could

be seen clearly. The force signals were sampled at 1 kHz, digitized with a 16-bit A/D converter, and stored on a PC.

After determination of the MVC, a rest period of 2 min was provided. Subsequently subjects performed a step contraction consisting of 10 force levels (5%–50% MVC with steps of 5%). Each step had to be maintained for 10 s. Between the levels, subjects relaxed their muscles and were allowed to start with the next level at their own pace. This resulted in interval rest periods of 10–20 s.

EMG Recordings. High-density sEMG of the biceps brachii muscle was recorded using a two-dimensional 16-channel array developed by the Helmholtz-Institute for Biomedical Engineering (Technical University Aachen, Aachen, Germany).¹⁵ The array consisted of four columns of gold-coated pin-electrodes with a diameter of 1.5 mm, the first and fourth containing three electrodes and the middle two containing five electrodes. The interelectrode distance was 10 mm in both directions.

Before electrode placement the skin was cleaned using abrasive paste. Electrode placement was done in accordance with the SENIAM (Surface Electromyography for the Non-Invasive Assessment of Muscles) recommendations for surface EMG recordings.³⁰ The electrode array was placed on the biceps brachii with the columns parallel to the line from the acromion to the cubital fossa, with the center of the array placed one-third of the distance from the cubital fossa. Signals were visually inspected online. Propagation of signals and minimal shape differences between subsequent signals were used as criteria for correct placement and alignment of the electrode columns in parallel to the muscle fibers. If necessary, the electrode array was repositioned. In most subjects a small amount of conducting gel was applied to the electrodes to improve the signal-to-noise ratio. A ground electrode was placed on the wrist.

The monopolar signals were amplified with a gain of 20, bandpass filtered (10–500 Hz), and 22-bits A/D-converted (resulting in a resolution of 71.5 nV per bit) with a 64-channel surface EMG amplifier (Twente Medical Systems International, Oldenzaal, the Netherlands), sample frequency 2,048 Hz, input resistance $>10^{12}$ Ohm, common mode rejection ratio >100 dB, noise <1 μ V RMS.

Data Analysis. All data were offline bandpass-filtered with a second-order zero phase shift Butterworth filter (10–400 Hz). For calculation of MUAP shape properties, bipolar signals with an interelec-

trode distance of 10 mm were constructed from the two middle columns of monopolar recorded signals. This resulted in two sets of four unidirectionally propagating bipolar signals. The set with the best signal quality was manually selected for further processing. Signals containing noise were discarded. For each subject at least three bipolar signals were available for MUAP detection.

MUAPs were detected with a method that uses the Continuous Wavelet Transform to identify shapes that were similar to a mother wavelet (i.e., the first-order Hermite–Rodriguez function). The algorithm separated the MUAPs from the surrounding background activity. The algorithm searched for candidate MUAPs on all channels. A candidate had to occur in at least three channels before being called an MUAP. The outcome of the detection algorithm was the MUAP shapes on all channels. A Hanning window was applied to smooth discontinuities at the start and end parts due to the extraction of the MUAPs. For more details about the detection algorithm, see previous studies.^{22,25,32}

Variables describing the MUAPs were calculated for all detected MUAPs without classifying them to their corresponding MU. The RMS value (RMS_{MUAP}) and the mean frequency of the power spectrum ($FMEAN_{MUAP}$) of each detected MUAP were calculated.³¹ Histograms of these variables were used to examine properties of the MU population. RMS_{MUAP} , related to the size of the MU, was calculated by taking the square root of the sum of all squared data samples of the MUAP, divided by the number of samples. $FMEAN_{MUAP}$ reflects the frequency content of the MUAP, which is related to the MUAP duration³⁰ and muscle fiber conduction velocity,^{3,17,34} which in turn is related to the recruitment threshold of the MU.¹ $FMEAN_{MUAP}$ was calculated as the mean value of the power spectrum, obtained using the fast Fourier-transform with a Hanning window. The MUAP shapes were zero-padded to obtain a frequency resolution of 1 Hz. $FMEAN_{MUAP}$ and RMS_{MUAP} were calculated from each of the four bipolar channels, and the values were averaged across the channels afterward. Ratios of $FMEAN_{MUAP}$ and RMS_{MUAP} on the affected side divided by the unaffected side were assessed to quantify within-subject differences between the sides.

For analysis of global surface EMG variables, three bipolar signals with an interelectrode distance of 2 cm were constructed from the monopolar signals by subtracting signals with 2 cm in between in the direction parallel to the muscle fibers, in accordance with the SENIAM guidelines for conventional surface EMG.³⁰ The signals were constructed from

the same set of monopolar signals as used for MUAP detection. The signals were inspected visually for the presence of artifacts and noise. Epochs containing artifacts were removed, and channels with noise were discarded. Global RMS (RMS_G) and median power frequency ($FMED_G$) were calculated from adjacent, nonoverlapping signal epochs of 1 s for each of the three signals. Average values across the three signals were calculated.

Statistics. Because the data were not normally distributed, nonparametric tests were used to assess differences in MVC and correlations between EMG variables. Differences in MVC between both sides were tested with the Wilcoxon signed-rank test for paired samples. Correlations between EMG variables were assessed using Spearman correlation coefficients, as were correlations between EMG variables and Fugl-Meyer scores. To investigate differences in EMG variables between the affected and the unaffected side, a mixed linear model was applied. Mixed linear models are designed to handle correlated data, including multiple observations of each subject. The model enables the inclusion of two sources of noise: one noise term for each subject, and one noise term for each measurement within a subject. Restricted maximum likelihood estimation was used for determining the factors that contributed significantly to the model. Quantitative changes in the EMG variables were estimated by applying the mixed model again with only the significant factors included.

The model included step (contraction level), side (affected or nonaffected), and the interaction of step with side as fixed factors. The interaction between step and side was included to examine differences between the sides in response to an increasing force level. Since it is known that body mass index (BMI) can have an effect on EMG variables,³⁸ BMI was included as a covariate. Furthermore, a random intercept for each subject was taken into account.

The residuals that the model generated were visually checked for normality. The only variable for which the residuals were not normally distributed was RMS_{MUAP} during the step contractions. Inspection of the data revealed one outlier with a value exceeding the 75th percentile plus three times the interquartile range. After removal of this subject the residuals were normally distributed.

RESULTS

The data from three subjects were discarded due to insufficient quality of the data of one side (two subjects) and absence of propagating MUAPs (one subject). In one subject, part of the data of the unaffected side was missing; the remaining data were included in the analysis. Three subjects were not able to perform the last step on one or both sides because of the high force level. In three subjects, for at least one side no MUAPs could be detected in step 1 and/or 2.

The maximal force was significantly lower (Wilcoxon signed-rank test, $P < 0.001$) on the affected side (median 118 N, range 29–329) than on the unaffected side (median 216 N, range 77–459) with a median ratio of 0.56 (affected divided by unaffected side).

Correlations between the EMG variables are reported in Table 2. For both sides the amplitude-related variables (RMS_{MUAP} and RMS_G) are strongly correlated, as are the frequency content-related variables ($FMEAN_{MUAP}$ and $FMED_G$). The EMG variables did not show a correlation with the Fugl-Meyer score.

An example of a recording of EMG signals of the affected and unaffected side is shown in Figure 1. In this subject the MUAPs were generally larger on the affected than on the unaffected side.

An example of the distribution of RMS_{MUAP} on the affected and unaffected sides is provided in Figure 2. Visual inspection of the histograms of all subjects showed that in 7 out of 15 subjects the

Table 2. Spearman's correlation coefficients.

Variable	RMS_G	RMS_{MUAP}	$FMED_G$	$FMEAN_{MUAP}$
RMS_G		0.971–0.991	NS	NS
RMS_{MUAP}	0.882–0.961		NS	NS
$FMED_G$	NS	NS		0.671–0.882
$FMEAN_{MUAP}$	NS	NS	0.664–0.896	

Parameters that showed significant correlation in at least five steps are presented. Ranges of correlation coefficients of all significant steps are presented. Upper right half shows minimal and maximal correlation coefficients for the unaffected side, lower left half shows the minimal and maximal correlation coefficients for the affected side. RMS_G : global root-mean-square value, RMS_{MUAP} : root-mean-square value of motor unit action potential, $FMED_G$: global median frequency of the power spectrum, $FMEAN_{MUAP}$: mean frequency of the power spectrum of motor unit action potential, NS: not significant.

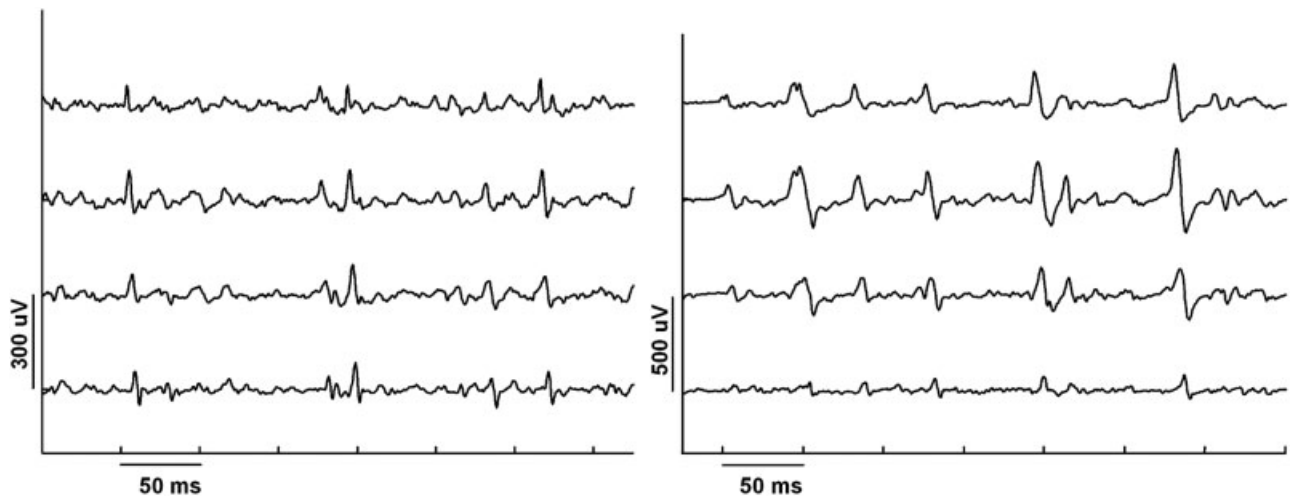


FIGURE 1. Example of high-density sEMG signals from the biceps brachii muscles of a stroke subject. Left: unaffected side; right: affected side. The contraction level was 25% of the maximum voluntary contraction force. Bipolar signals from one column of a 16-channel electrode array are shown. Note the different amplitude scales.

MUAPs were larger on the affected than on the unaffected side, with a broader distribution (example at the left side of Fig. 2). In five subjects the MUAPs were smaller, and the distribution was more narrow (example on the right side of Fig. 2). In the remaining three subjects no clear differences between the two sides were found. For all subjects together the statistical model revealed a trend for higher RMS_{MUAP} values on the affected side (difference of $11.02 \mu V$, $P < 0.10$), but the increase of RMS_{MUAP} with force level was smaller ($5.7 \mu V$ vs. $7.9 \mu V$ per step). The standard deviation of RMS_{MUAP} also increased less with step on the affected side (3.79 vs. $5.30 \mu V$ per step). The results for RMS_G were comparable.

Interestingly, the Fugl-Meyer scores in the subjects with larger MUAPs on the affected side tended to be higher than those in the subjects with smaller MUAPs (median values and ranges 20 [19–53] and 42 [21–62], respectively, $P < 0.071$, Mann–Whitney U -test). Figure 3 shows a scatterplot of RMS_{MUAP} ratio (RMS_{MUAP} of the affected side divided by that of the unaffected side) and Fugl-Meyer score. For all steps except for steps 1, 2, and 10 there was a significant correlation with Spearman's rho between 0.60 and 0.74 ($P = 0.006$ – 0.039). On average, 42% of the variance in the Fugl-Meyer score was explained by the RMS_{MUAP} ratio. RMS_G ratio and Fugl-Meyer score were significantly correlated for the same steps, with Spearman's rho between 0.55 and 0.65 ($P = 0.009$ – 0.035) and, on average, an explained variance of 34%.

An example of the distribution of $FMEAN_{MUAP}$ on the affected and unaffected side is provided in Figure

4. In this subject the MUAPs on the affected side have a lower mean frequency of the power spectrum than the MUAPs on the unaffected side. Visual inspection showed that this was the case in 7 out of 15 subjects. In six subjects the distributions of the affected and unaffected sides were not different and in the remaining two subjects the MUAPs on the affected sides showed higher $FMEAN_{MUAP}$ values. For all subjects together the statistical model revealed that $FMEAN_{MUAP}$ was lower on the affected than on the unaffected side (108 vs. 114 Hz, $P < 0.001$). There was a small but statistically significant decrease of $FMEAN_{MUAP}$ with force (0.77 Hz per step, $P < 0.001$). $FMED_G$ did not show a significant difference in mean value between the two sides, but $FMED_G$ increased slightly on the unaffected side with force (0.40 Hz per step, $P < 0.002$), while it decreased slightly on the affected side (0.46 Hz per step, $P < 0.002$).

DISCUSSION

The aim of this study was to investigate MU characteristics in stroke subjects. The results showed a lower mean frequency of the power spectrum of the MUAPs on the affected side. Furthermore, in seven subjects the MUAPs were larger on the affected side, while in five subjects the MUAPs were smaller. A correlation was found between a clinical scale, the Fugl-Meyer score, and the ratio of RMS_{MUAP} on the affected divided by the unaffected side.

The subject population had a median upper extremity Fugl-Meyer score of 35.5. Boissy et al. (1997) used a cutoff point of 44 to divide a group of stroke patients into moderately (>44) and severely (≤ 44)

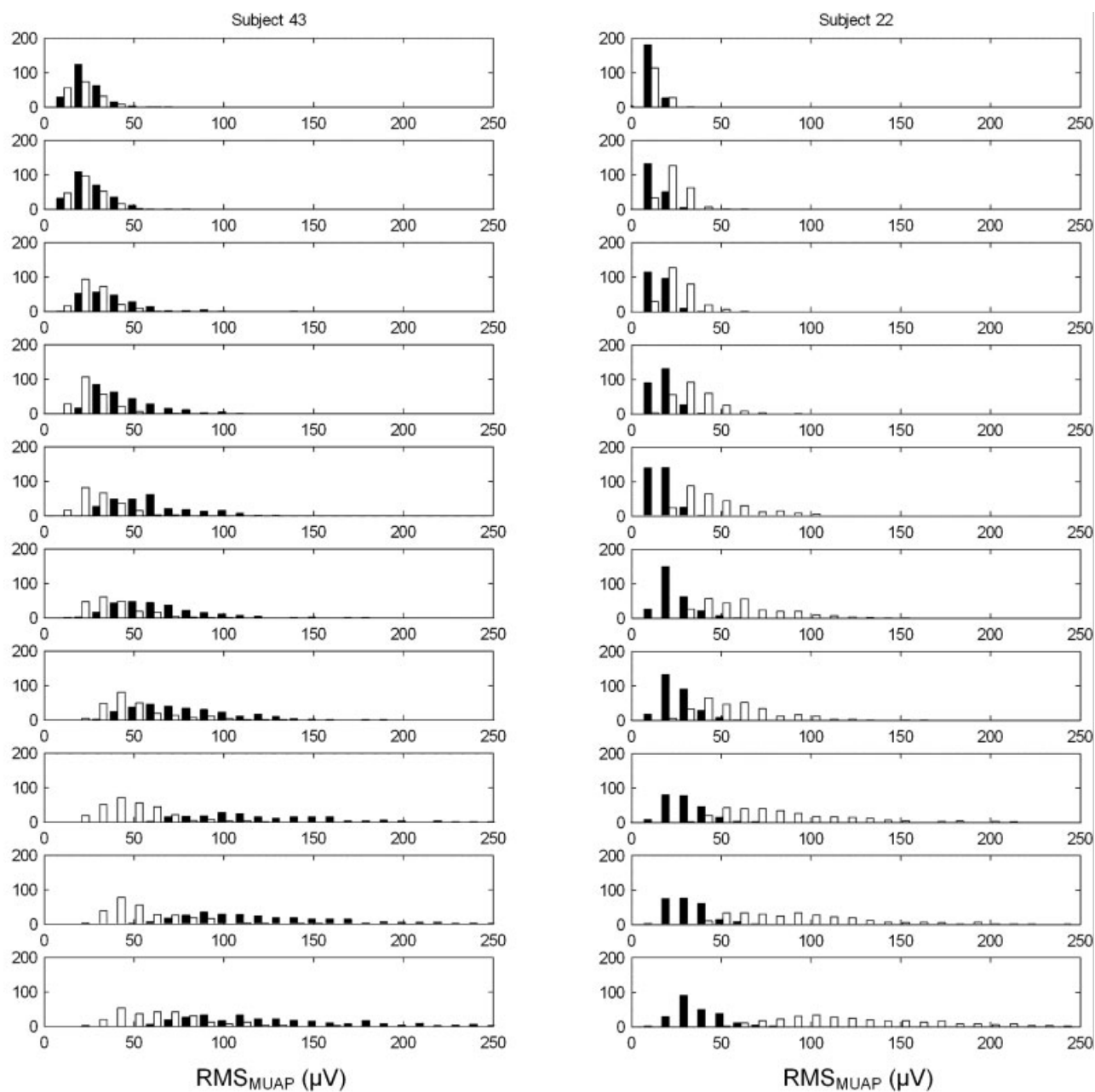


FIGURE 2. Histograms of RMS_{MUAP} of two stroke subjects, representative of two subgroups of subjects. Each histogram represents one contraction level; from 5% MVC (upper graphs) to 50% MVC (lower graphs). In the first subgroup (left), RMS_{MUAP} values of the affected side are larger and more variable than those of the unaffected side. In the other subgroup (right) the RMS_{MUAP} values of the affected side are smaller and less variable. Filled bars: affected side; open bars: unaffected side.

affected patients.⁵ According to this cutoff point, on average the population in this study can be classified as severely affected. The range of Fugl-Meyer values was large (from 9 to 62), which reflects the large variability of the group.

The MVC value of the affected side was approximately twice as low as that of the unaffected side. A similar decrease in force on the affected side (aver-

age ratio of 0.48) was found before in a study assessing muscle force in stroke subjects.²

For each side separately, no correlation between the EMG variables and Fugl-Meyer score was found. However, the ratio of RMS_{MUAP} of the affected side, divided by the unaffected side, showed a moderately strong relation with the Fugl-Meyer score. A larger RMS_{MUAP} value indicates that the size of the MUAP

as recorded on the skin is larger, which is related to larger MUs.³³ Although the present data are not conclusive, this is in agreement with findings of electrophysiological studies and has been suggested to be caused by the occurrence of reinnervation of muscle fibers by collateral sprouting and branching.^{11,29,36} Therefore, the RMS_{MUAP} ratio might reflect the amount of reinnervation, which is a compensation strategy for paresis and, as such, is likely to be related to the functional capacity of the muscle.

The unaffected arm may differ from the arm of a healthy subject. For example, compensation strategies might result in overuse of the unaffected side. This could lead to an increase in fiber diameter on the unaffected side, in which case RMS_{MUAP} of the unaffected side would increase. This would make the RMS_{MUAP} ratio lower. One could argue that overuse occurs to a larger extent when there is little recovery of the affected side. This could be a complementary explanation for the correlation between the RMS_{MUAP} ratio and Fugl-Meyer score.

In contrast to the ratio, RMS_{MUAP} of each side separately does not correlate with the Fugl-Meyer score. Taking the ratio of the affected side divided by the unaffected side might decrease the effect of subject-specific characteristics such as subcutaneous tissue or MVC force, thereby decreasing intersubject variability. Furthermore, the Fugl-Meyer score is also a comparison of the affected side with the unaffected side.

Besides size of the MU, RMS_{MUAP} is also related to the distance between the MU and the recording site. When the subcutaneous tissue is thicker, lower

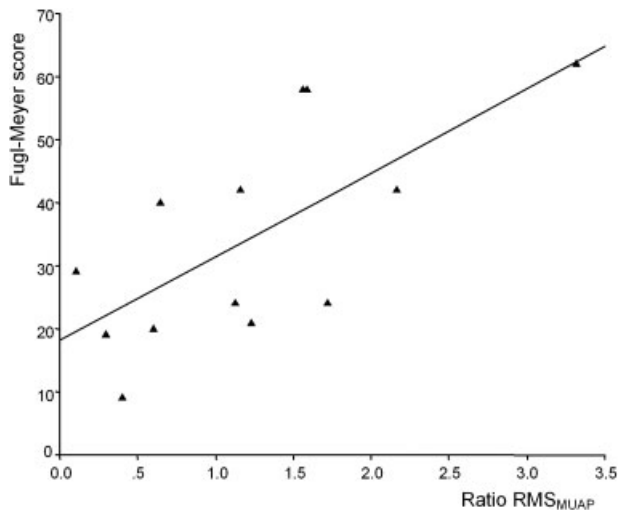


FIGURE 3. Scatterplot of the ratio of RMS_{MUAP} on the affected side divided by RMS_{MUAP} on the unaffected side against Fugl-Meyer score. Data from step 6 (30% MVC). The explained variance is 47% ($P < 0.011$).

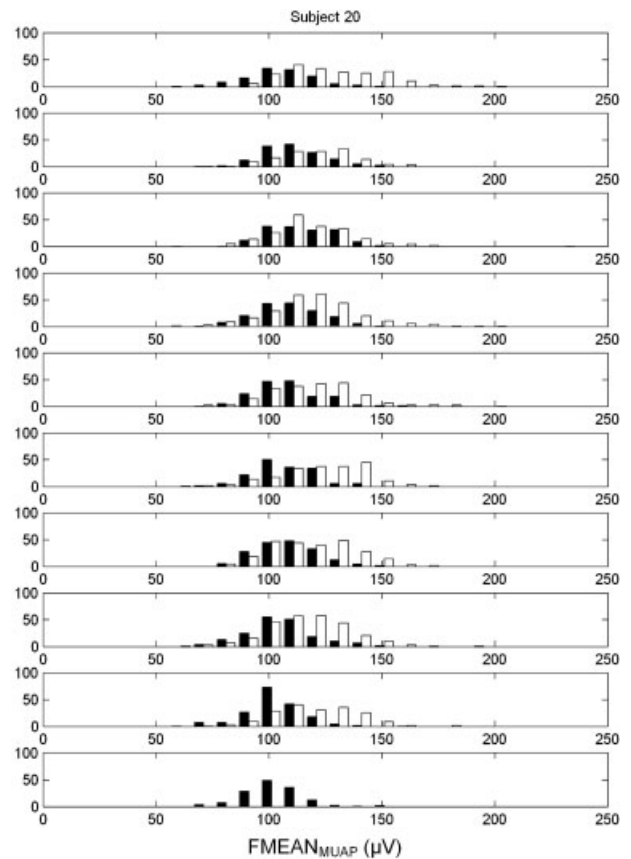


FIGURE 4. Histograms of $FMEAN_{MUAP}$ of one subject of the affected and unaffected side during the 10 contraction levels. Each histogram represents one contraction level: from 5% MVC (upper graphs) to 50% MVC (lower graphs). Filled bars: affected side; open bars: unaffected side. Data of unaffected side are missing for the last contraction level.

RMS_{MUAP} values are recorded. To compensate for this effect BMI was included as a covariate in the statistical analysis, and ratios of the affected side divided by the unaffected side were used.

The frequency content of the MUAP (measured with $FMEAN_{MUAP}$) is related to its duration³¹ and to the muscle fiber conduction velocity,^{4,18,35} which in turn is related to the recruitment threshold of the MU.¹ The lower $FMEAN_{MUAP}$ values at the affected side might point at muscle atrophy, resulting in a smaller fiber diameter, directly leading to a lower conduction velocity. Additionally, it might indicate a larger contribution of low-threshold MUs. This might be explained by transsynaptic degeneration; it has been shown that mainly type II MUs (generally high-threshold) are affected by degeneration,^{6,9,11,14,26,37,43} while type I MUs (generally low-threshold) remain, which would increase the relative contribution of low-threshold MUs. This effect might be enhanced by

collateral sprouting of the remaining low-threshold MUs, as has been suggested by different authors.^{10,29}

In contrast to $FMEAN_{MUAP}$, $FMED_C$ did not show differences between the two sides. This might point to a higher sensitivity of MUAP variables, which was found previously.^{32,34}

In conclusion, high-density sEMG recordings of chronic stroke patients revealed differences in MUAP size and in frequency content of the MUAPs between the affected and the unaffected side. The ratio of RMS_{MUAP} on the affected side divided by that of the unaffected side correlated significantly with the Fugl-Meyer score for the upper extremity. This ratio may reflect the extent to which reinnervation has occurred on the affected side. The smaller values of $FMEAN_{MUAP}$ on the affected side might point to an increased relative contribution of low-threshold MUs, possibly related to degeneration of high-threshold MUs.

The authors thank Marjon Nijboer, MSc, PT, for help with the data collection and Bertjo Renzenbrink, PhD, MD, for help with the study design and patient recruitment. This study was partially funded by the Dutch Ministry of Economical Affairs.

REFERENCES

1. Andreassen S, Arendt-Nielsen L. Muscle fibre conduction velocity in motor units of the human anterior tibial muscle: a new size principle parameter. *J Physiol* 1987;391:561–571.
2. Andrews AW, Bohannon RW. Distribution of muscle strength impairments following stroke. *Clin Rehabil* 2000;14:79–87.
3. Arendt-Nielsen L, Mills KR. The relationship between mean power frequency of the EMG spectrum and muscle fibre conduction velocity. *Electroencephalogr Clin Neurophysiol* 1985;60:130–134.
4. Bohannon RW, Smith MB. Interrater reliability of a modified Ashworth scale of muscle spasticity. *Phys Ther* 1987;67:206–207.
5. Boissy P, Bouibonnais D, Kaegi C, Gravel D, Arseneault BA. Characterization of global synkinesis during hand grip in hemiparetic patients. *Arch Phys Med Rehabil* 1997;78:117–1124.
6. Brooke MH, Engel WK. The histographic analysis of human muscle biopsies with regard to fiber types. 2. Diseases of the upper and lower motor neuron. *Neurology* 1969;19:378–393.
7. Chae J, Yang G, Park BK, Labatia I. Delay in initiation and termination of muscle contraction, motor impairment, and physical disability in upper limb hemiparesis. *Muscle Nerve* 2002;25:568–575.
8. Chae J, Yang G, Park BK, Labatia I. Muscle weakness and cocontraction in upper limb hemiparesis: relationship to motor impairment and physical disability. *Neurorehabil Neural Repair* 2002;16:241–248.
9. Chokroverty S, Reyes MG, Rubino FA, Barron KD. Hemiplegic amyotrophy. Muscle and motor point biopsy study. *Arch Neurol* 1976;33:104–110.
10. Cruz Martinez A, del Campo F, Mingo MR, Perez Conde MC. Altered motor unit architecture in hemiparetic patients. A single fibre EMG study. *J Neurol Neurosurg Psychiatry* 1982;45:756–757.
11. Dattola R, Girlanda P, Vita G, Santoro M, Roberto ML, Toscano A, et al. Muscle rearrangement in patients with hemiparesis after stroke: an electrophysiological and morphological study. *Eur Neurol* 1993;33:109–114.
12. Dewald JP, Beer RF, Given JD, McGuire JR, Rymer WZ. Reorganization of flexion reflexes in the upper extremity of hemiparetic subjects. *Muscle Nerve* 1999;22:1209–1221.
13. Dewald JP, Pope PS, Given JD, Buchanan TS, Rymer WZ. Abnormal muscle coactivation patterns during isometric torque generation at the elbow and shoulder in hemiparetic subjects. *Brain* 1995;118(Pt 2):495–510.
14. Dietz V, Ketelsen UP, Berger W, Quintern J. Motor unit involvement in spastic paresis. Relationship between leg muscle activation and histochemistry. *J Neurol Sci* 1986;75:89–103.
15. Disselhorst-Klug C, Bahm J, Ramaekers V, Trachterna A, Rau G. Non-invasive approach of motor unit recording during muscle contractions in humans. *Eur J Appl Physiol* 2000;83:144–150.
16. Drost G, Stegeman DF, Schillings ML, Horemans HL, Janssen HM, Massa M, et al. Motor unit characteristics in healthy subjects and those with postpoliomyelitis syndrome: a high-density surface EMG study. *Muscle Nerve* 2004;30:269–276.
17. Drost G, Stegeman DF, van Engelen BG, Zwarts MJ. Clinical applications of high-density surface EMG: a systematic review. *J Electromyogr Kinesiol* 2006;16:586–602.
18. Dumitru D, King JC, Zwarts MJ. Determinants of motor unit action potential duration. *Clin Neurophysiol* 1999;110:1876–1882.
19. Edstrom L. Selective changes in the sizes of red and white muscle fibres in upper motor lesions and Parkinsonism. *J Neurol Sci* 1970;11:537–550.
20. Falla D, Jull G, Rainoldi A, Merletti R. Neck flexor muscle fatigue is side specific in patients with unilateral neck pain. *Eur J Pain* 2004;8:71–77.
21. Farina D, Cescon C, Merletti R. Influence of anatomical, physical, and detection-system parameters on surface EMG. *Biol Cybern* 2002;86:445–456.
22. Farina D, Fortunato E, Merletti R. Noninvasive estimation of motor unit conduction velocity distribution using linear electrode arrays. *IEEE Trans Biomed Eng* 2000;47:380–388.
23. Farina D, Gazzoni M, Merletti R. Assessment of low back muscle fatigue by surface EMG signal analysis: methodological aspects. *J Electromyogr Kinesiol* 2003;13:319–332.
24. Fugl-Meyer AR, Jaasko L, Leyman I, Olsson S, Stegling S. The post-stroke hemiplegic patient. I. a method for evaluation of physical performance. *Scand J Rehabil Med* 1975;7:13–31.
25. Gazzoni M, Farina D, Merletti R. A new method for the extraction and classification of single motor unit action potentials from surface EMG signals. *J Neurosci Methods* 2004;136:165–177.
26. Goldkamp O. Electromyography and nerve conduction studies in 116 patients with hemiplegia. *Arch Phys Med Rehabil* 1967;48:59–63.
27. Hammond MC, Fitts SS, Kraft GH, Nutter PB, Trotter MJ, Robinson LM. Co-contraction in the hemiparetic forearm: quantitative EMG evaluation. *Arch Phys Med Rehabil* 1988;69:348–351.
28. Hammond MC, Kraft GH, Fitts SS. Recruitment and termination of electromyographic activity in the hemiparetic forearm. *Arch Phys Med Rehabil* 1988;69:106–110.
29. Hara Y, Masakado Y, Chino N. The physiological functional loss of single thenar motor units in the stroke patients: when does it occur? Does it progress? *Clin Neurophysiol* 2004;115:97–103.
30. Hermens HJ, Freriks B, Disselhorst-Klug C, Rau G. Development of recommendations for SEMG sensors and sensor placement procedures. *J Electromyogr Kinesiol* 2000;10:361–374.
31. Hermens HJ, van Bruggen TAM, Baten CTM, Rutten WLC, Boom HBK. The median frequency of the surface EMG power spectrum in relation to motor unit firing and action potential properties. *J Electromyogr Kinesiol* 1992;2:15–25.
32. Kallenberg LAC, Hermens HJ. Motor unit action potential rate and motor unit action potential shape properties in

- subjects with work-related chronic pain. *Eur J Appl Physiol* 2006;96:203–208.
33. Kallenberg LAC, Hermens HJ. Behaviour of motor unit action potential rate, estimated from surface EMG, as a measure of muscle activation level. *J Neuroengineering Rehabil* 2006; 3:15.–
 34. Kallenberg LAC, Hermens HJ, Vollenbroek-Hutten MM. Distinction between computer workers with and without work-related neck-shoulder complaints based on multiple surface EMG parameters. *Int J Industr Ergon* 2006;36:921–929.
 35. Lindstrom LH, Magnusson RI. Interpretation of myoelectric power spectra: a model and its applications. *IEEE Trans Biomed Eng* 1977;65:653–662.
 36. Lukacs M. Electrophysiological signs of changes in motor units after ischaemic stroke. *Clin Neurophysiol* 2005;116:1566–1570.
 37. McComas AJ, Sica RE, Upton AR, Aguilera N. Functional changes in motoneurons of hemiparetic patients. *J Neurol Neurosurg Psychiatry* 1973;36:183–193.
 38. Merletti R, Farina D, Gazzoni M. The linear electrode array: a useful tool with many applications. *J Electromyogr Kinesiol* 2003;13:37–47.
 39. Nordander C, Willner J, Hansson GA, Larsson B, Unge J, Granquist L, et al. Influence of the subcutaneous fat layer, as measured by ultrasound, skinfold calipers and BMI, on the EMG amplitude. *Eur J Appl Physiol* 2003;89:514–519.
 40. Ramaekers VT, Disselhorst-Klug C, Schneider J, Silny J, Forst J, Forst R, et al. Clinical application of a noninvasive multi-electrode array EMG for the recording of single motor unit activity. *Neuropediatrics* 1993;24:134–138.
 41. Rau G, Schulte E, Disselhorst-Klug C. From cell to movement: to what answers does EMG really contribute? *J Electromyogr Kinesiol* 2004;14:611–617.
 42. Roeleveld K, Stegeman DF. What do we learn from motor unit action potentials in surface electromyography? *Muscle Nerve* 2002;11 (Suppl):S92–97.
 43. Scelsi R, Lotta S, Lommi G, Poggi P, Marchetti C. Hemiplegic atrophy. Morphological findings in the anterior tibial muscle of patients with cerebral vascular accidents. *Acta Neuropathol* 1984;62:324–331.
 44. Schulte E, Farina D, Rau G, Merletti R, Disselhorst-Klug C. Single motor unit analysis from spatially filtered surface electromyogram signals. Part 2: conduction velocity estimation. *Med Biol Eng Comput* 2003;41:338–345.
 45. Staudenmann D, Kingma I, Daffertshofer A, Stegeman DF, van Dieen JH. Improving EMG-based muscle force estimation by using a high-density EMG grid and principal component analysis. *IEEE Trans Biomed Eng* 2006;53:712–719.
 46. Toffola ED, Sparpaglione D, Pistorio A, Buonocore M. Myoelectric manifestations of muscle changes in stroke patients. *Arch Phys Med Rehabil* 2001;82:661–665.
 47. Young JL, Mayer RF. Physiological alterations of motor units in hemiplegia. *J Neurol Sci* 1982;54:401–412.